Published in final edited form as:

Nature. 2008 December 11; 456(7223): 755–761. doi:10.1038/nature07513.

Fus3 generates negative feedback that improves information transmission in yeast pheromone response

Richard C. Yu, **C. Gustavo Pesce**, **Alejandro Colman-Lerner**[2], **Larry Lok**[3], **David Pincus**[4], **Eduard Serra**[5], **Mark Holl**[1,6], **Kirsten Benjamin**[7], **Andrew Gordon**[8], and **Roger Brent**

Molecular Sciences Institute, 2168 Shattuck Avenue, Berkeley, California 94704 USA

[1] Microscale Life Sciences Center, University of Washington, Seattle, Washington 98195 USA

Abstract

Haploid *Saccharomyces cerevisiae* yeast cells use a prototypic cell signaling system to transmit information about the extracellular concentration of mating pheromone secreted by potential mating partners. The ability for cells to respond distinguishably to different pheromone concentrations depends on how much information about pheromone concentration the system can transmit. Here we show that the MAPK Fus3 mediates fast-acting negative feedback that adjusts the dose-response of downstream system response to match that of receptor-ligand binding. This "dose-response alignment", defined by a linear relationship between receptor occupancy and downstream response, can improve the fidelity of information transmission by making downstream responses corresponding to different receptor occupancies more distinguishable and reducing amplification of stochastic noise during signal transmission. We also show that one target of the feedback is a novel signal-promoting function of the RGS protein Sst2. Our work suggests that negative feedback is a general mechanism used in signaling systems to align dose-responses and thereby increase the fidelity of information transmission.

Correspondence and requests for materials should be addressed to ryu@molsci.org and brent@molsci.org.
[2]Instituto de Fisiología, Biología Molecular y Neurociencias, CONICET and Departamento de Fisiología, Biología Molecular y Celular, Facultad de Ciencias Exactas y Naturales, Universidad de Buenos Aires, Argentina
[3]Synopsys, Mountain View, CA 94043, USA
[4]Department of Cellular and Molecular Pharmacology, University of California, San Francisco 94158, USA
[5]Centre de Genètica Mèdica i Molecular, Institut d'Investigació Biomèdica de Bellvitge (IDIBELL), Barcelona, Spain
[6]Biodesign Institute, Arizona State University, Tempe, Arizona 85387, USA
[7]Amyris Biotechnologies, Emeryville, California 94608, USA
[8]Physics Department, Brookhaven National Laboratory, Upton, New York 11973 USA

Author contributions

R.Y. performed the Ste5 translocation, loss of G-protein and Dig1/Ste12 FRET, MAP kinase phosphorylation, mRNA measurements, and the image-based measurements of system output. G.P. and A.G. noted and helped articulate the relationship of negative feedback to dose response overlap. G.P. and R.Y. performed flow cytometric measurements. L.L. and A.G. contributed to valuable discussions about mutual information calculations and analysis. R.Y. and A.G. performed data analysis on loss of FRET experiments. A.C.-L. and A.G. carried out extensive initial measurements of Ste5 recruitment. K.B. provided unpublished information about protein quantification useful in initial discussions about dose-response alignment. R.Y. and D.P. performed numerous measurements verifying protein abundance in other strains. E.S. constructed the inhibitor-sensitive *fus3-as2* and *kss1-as2* alleles. M.H. designed and built fluidic devices used to induce the system in response to articulated requirements. R.B. provided input into project direction, experimental design, and interpretation of results. R.Y., G.P. and R.B. wrote the paper and guarantee the integrity of the results.

Author information

Background and results

Cells use signaling systems to sense and transmit information about extracellular conditions. Haploid *Saccharomyces cerevisiae* yeast cells use a prototypic, G-protein coupled-receptor/MAP kinase cascade signaling system, the pheromone response system 1, to sense and transmit information about the concentration of mating pheromone secreted by cells of the opposite mating type (Fig. 1). The more information about pheromone concentration the system can transmit, the better a cell can distinguish between different pheromone concentrations, an essential ability for proper partner choice and mating. For example, a yeast cell ringed by potential mating partners strongly prefers to mate with partners producing the most pheromone 2. Partner choice involves two processes that require sensing of pheromone concentration. First, a cell grows up the pheromone concentration gradient 3, a process that likely depends on measurement of precise differences in pheromone concentration at different points on the cell surface. Second, after contacting its partner and forming a prezygote, a cell preferentially completes fusion and forms a diploid with a partner that produces high amounts of pheromone 4. These experiments indicate it is important for cells to distinguish among different pheromone concentrations at multiple steps during the mating process.

Prior work suggested that optimal transmission of information about pheromone concentration depends on both distinguishable receptor occupancies and distinguishable downstream system responses. Differences in receptor occupancy are clearly important for mating partner choice and discrimination; for example, in the presence of exogenous pheromone at a concentration that saturates the receptor, cells lose the ability to discriminate high pheromone-secreting partners from low pheromone-secreting partners 2. However, distinguishable receptor occupancies are not sufficient for partner discrimination, since hypersensitive cells, in the presence of exogenous pheromone at a concentration that does not saturate the receptor but does saturate downstream responses, also lose the ability to discriminate between partners secreting different levels of pheromone 2. In complementary studies of orientation of mating projections in spatial gradients of pheromone, Segall 3 showed that hypersensitive cells did not orient their mating projections as precisely as wild-type cells and suggested that this might result from saturation of downstream responses at most points in the gradient. However, after reducing the gradient pheromone concentrations 100 fold to concentrations at which downstream responses are not predicted to be saturated, hypersensitive cells oriented their mating projections less precisely than wild-type cells orient in gradients of higher pheromone concentrations 3. These observations suggest that hypersensitive cells are inherently less able to respond distinguishably to different pheromone concentrations (i.e., transmit less information about pheromone concentration), even when they are responding to pheromone concentrations that saturate neither receptor nor downstream responses.

DoRA increases response distinguishability

One characteristic of wild-type cells that we 5 and others 6 have previously found is that, despite the large number of intermediate signaling events in the system, the dose-response curve of receptor occupancy closely aligns with dose-responses curves of downstream

system responses. For example, we observe “dose-response alignment” (here called DoRA) between receptor occupancy and the amount of pheromone-activated Ste12 (pathway subsystem output *P*, which is reporter gene expression corrected for inherent cell-to-cell differences in the ability to express proteins 5) (Fig. 2a). Interestingly, dose-response alignment is commonly observed in many mammalian cell signaling systems, including the insulin 7, acetylcholine 8, thyroid stimulating hormone 9, angiotensin II 10, and epidermal growth factor 11,12 response systems. Researchers in the past have often regarded alignment of curves for ligand binding by a candidate receptor and downstream response as evidence that the putative receptor was in fact the molecule that bound ligand and caused the cellular responses13–15. However, to our knowledge, researchers have investigated neither the implications of dose-response alignment for yeast pheromone response nor its general consequences for the function of cell signaling systems.

We realized that dose-response alignment improves information transmission in two ways. First, DoRA describes a linear relationship between receptor occupancy and downstream response; consequently, the entire range of receptor occupancies evenly corresponds to the entire range of possible responses (Fig. 2b). By contrast, even a modest dose-response misalignment, such as a 20-fold shift in the EC50 of downstream response (Fig. 2c), compresses the downstream responses corresponding to a wide range of receptor occupancies into a narrow range (Fig. 2d). Second, dose-response alignment minimizes the amplification of upstream noise (Fig. 2e). Previous analysis of noise propagation in a synthetic gene circuit revealed analogous amplification of upstream noise in a system with misaligned dose-responses16. This reasoning suggested to us that cell signaling systems with misaligned dose-responses inherently transmit information with lower fidelity, even if downstream responses are not saturated, an idea consistent Segall’s observations that hypersensitive cells oriented mating projections less precisely in gradients than wild-type cells even at concentrations that did not saturate downstream responses 3. We hypothesized that dose-response alignment might indicate a system that can transmit large amounts of information, and therefore we sought to better understand the underlying molecular mechanisms required for DoRA and the linear relationship between upstream and downstream response that it defines.

In the 1930s, Harold Black established that “proportional” negative feedback in electrical circuits, where a constant fraction of the output is subtracted from the input, can bring about a linear input-output voltage relationship17. Biologists have also shown that negative feedback can make input-output relationships more linear in biological systems; for example, Bhalla *et al*. showed that, in a MAPK/PKC-mediated signaling system, increasing the amount of a MAPK-activated phosphatase that inactivates the MAPK made the average output response more linearly related to (i.e., proportional to) the input18. Research in both biology and engineering 17,19–22 has also suggested or shown that negative feedback can increase the signal-to-noise ratio in system output and decrease the sensitivity of output to variation in properties of system components (see Supplementary Information 8 for further discussion). These observations suggested to us that negative feedback might mediate dose-response alignment and improve information transmission in the yeast pheromone response system.

Prior work showed that the pheromone response system quickly establishes dose-response alignment; the accumulation of reporter gene expression in cells increased linearly from 15 minutes to three hours after stimulation (see Fig. 2 in 5), and at all times the normalized dose-response of downstream output aligned with the receptor-ligand binding curve. These facts suggested that the molecular mechanisms that bring about and stabilize DoRA occurs in the first 15 minutes of pheromone stimulation. However, no quantitative measurements of system activities in this time frame existed to indicate the action of negative feedback to align dose-responses. We therefore developed tools to measure the early dynamics of molecular events that the system uses to operate before, during, and after establishment of DoRA.

Initial system dynamics indicate negative feedback

We developed reporters and methods to measure real-time signal transmission in single cells, at the membrane, and in the nucleus, and supplemented these data with biochemical measurements. We then measured system outputs (i.e., system activities at different stages in the signaling pathway, see Fig. 1) after stimulating cells with 100 nM pheromone, a concentration that produces maximal downstream transcription reporter response (Fig. 2a).

Two membrane-proximal system outputs, G-protein activation and Ste5 recruitment to the membrane, peaked and declined rapidly. To follow G-protein activation in single cells over time, we measured loss of Fluorescence Resonance Energy Transfer (FRET) between cyan fluorescent protein (CFP)-tagged Gpa1 and yellow fluorescent protein (YFP)-tagged Ste18 by image cytometry 23 (Supplementary Information 2) in a derivative of a strain developed by Yi and coworkers6. Loss of G-protein FRET rapidly peaked in the first minute and declined (Fig. 3a and Fig. S2), consistent with lower time resolution, single time point population measurements in an earlier study 6.

We then measured, also in single cells and at sub-minute intervals, a subsequent membrane-proximal signaling event, the recruitment of Ste5 to the membrane. To do this, we measured the redistribution of YFP-Ste5 from the nucleus and cytosol to the membrane (Supplementary Information 2). Membrane recruitment of Ste5 was rapid (Fig 3b). Within 5 seconds of stimulation with high pheromone, individual cells showed an increase in yellow fluorescence at the cell membrane, and a corresponding depletion of fluorescence from the cell interior; no change in fluorescence was observed in unstimulated cells or cells with unlabeled Ste5 (Fig. S3). Compared with unstimulated cells, average membrane recruitment reached near-maximal values within seconds and peaked by 20 seconds, before declining toward a plateau in later minutes, similar to the dynamics of G-protein loss of FRET.

We then assessed intermediate system output further downstream by measuring the dynamics of MAPK activation. Using quantitative immunoblotting, we measured phosphorylation of Fus3 residues Thr180 and Tyr182, which is required for Fus3 activity and pheromone response 24. The amount of phosphorylated Fus3 relative to total Fus3 increased rapidly, reaching a maximum in 2.5 min before dropping to a plateau level in approximately 5–7 min (Fig. 3c and Fig. S4a–b).

We then measured nuclear MAPK activity dynamics in single cells over time. To do this, we developed a FRET reporter to measure pheromone-induced changes in the association between the transcription factor Ste12 and one of its inhibitors Dig1 25. We deleted native *STE12* and *DIG1* genes and chromosomally integrated versions of these proteins fused to CFP and YFP, respectively (see Supplementary Information 5). We then measured changes in FRET between CFP and YFP 26 in the nucleus by image cytometry 23 (see Fig. S6 and Supplementary Information 2). Pheromone-induced loss of FRET did not require new protein translation (Fig. S7b), but did require both Ste5 (Fig S7c) and MAP kinase activity (Fig S7d), consistent with the interpretation that loss of FRET directly reported pheromone-induced, MAP kinase-mediated derepression of Ste12.

Loss of Dig1-Ste12 FRET quickly peaked around 3 min after stimulation (Fig. 3d), and the overall signal dynamics were very similar to those of Fus3 phosphorylation (compare Fig. 3c to Fig. 3d, see also Fig. 3f). This fast signal transfer from Fus3 activation to Ste12 derepression is consistent with the idea that Fus3 moves quickly in and out of the nucleus, as shown in studies of changes in Fus3 localization by fluorescence recovery after photobleaching (FRAP)27. We confirmed that the timing of Ste12 de-repression measured by loss of Ste12-Dig1 FRET was consistent with the dynamics of pheromone-induced mRNA transcription. Using ribonuclease protection assays, we quantified *FUS1* mRNA levels. *FUS1* mRNA levels peaked at 5 minutes following pheromone stimulation before declining (Fig. 3e and Fig. S8). The maximum rate of increase in mRNA occurred between 3 and 5 minutes, consistent with the time of maximum loss of Ste12-Dig1 FRET.

All measurements of signal-relaying events showed a consistent pattern of rapid peak-and-decline toward a plateau after pheromone stimulation (Fig. 3f), which suggested the action of one or more fast-acting negative feedbacks that might modulate the dose-dependence of the signal to achieve DoRA.

Fus3 mediates negative feedback

A number of previous works suggested that the MAPKs Fus3 and Kss1 might mediate rapid negative feedback. Our previous study of regulated cell-to-cell variation in system output revealed a Fus3-dependent reduction in variation, suggesting an autoregulatory negative feedback mediated by Fus3 5. Gartner et al. showed that levels of phosphorylated Fus3 were higher in cells bearing a kinase-dead mutant version of Fus324. Bhattacharya et al. showed that Ste5 T287A mutant cells, in which the Ste5 carries a lesion in a site of threonine phoshorylated by Fus3 on peptides *in vitro* exhibited increased reporter expression 28, albeit with no change in the EC50 of the dose-response. Finally, phosphoproteomic studies of pheromone response system proteins29 have uncovered numerous sites of phosphorylation on pheromone response system proteins, whose levels change upon pheromone stimulation, many of which lie in consensus MAP kinase target sequences (R. Maxwell and O. Resnekov, personal communication). We therefore hypothesized that the signal decline at different measurement points depends on non-translational, fast-acting negative feedbacks mediated by Fus3 or Kss1.

To test if Fus3 or Kss1 were sources of negative feedback on system activity, we compared the baseline system response, at system points up to and including Fus3 phosphorylation, with system response after selective inhibition of either Fus3 or Kss1 kinase activity. To do this, we first modified reporter strains by replacing either *FUS3* or *KSS1* with the corresponding purine analog-sensitive allele 30. We did this by changing the "gatekeeper" residue in each kinase's ATP binding pocket (Q93 in Fus3, N94 in Kss1) to an alanine. The mutant *fus3-as2* and *kss1-as2* kinases were active, as measured by fluorescent protein reporter gene output (Fig. S9a), and10 μM 1-NM-PP1, a cell-permeable adenosine analogue, inhibited the activity of mutant kinases without inhibiting wild-type kinases (Fig. S9b). We then quantified Fus3 phosphorylation by quantitative immunoblotting after stimulation with pheromone, either with or without simultaneous inhibition with 1-NM-PP1 (Fig. 4a). Fus3 phosphorylation levels did not peak and decline to a plateau when we inhibited Fus3-as2, but, rather, remained high, near peak levels. By contrast, when we inhibited Kss1-as2, Fus3 phosphorylation levels were unaffected (Fig. 4b). These results indicated that Fus3 kinase activity mediated one or more negative feedbacks in this system.

We then studied where in the system the Fus3-dependent feedback acted to diminish signal amplitude. Yi et al. showed that the decrease in G-protein FRET within 30 seconds of stimulation depended on Sst2 6. This finding suggested that the Fus3-dependent negative feedback might upregulate the GTPase-activating protein (GAP) function of Sst2, which would increase G protein reassociation and decrease downstream signal. We tested if Fus3-as2 inhibition affected the observed decline in both G-protein dissociation and Ste5 recruitment. Inhibition of Fus3 activity eliminated the decline in Ste5 translocation (Fig. 4c), but surprisingly had no effect on the decline in G-protein dissociation in a G-protein FRET reporter strain carrying *fus3-as2* (Fig. 4d and Fig. S10). These results indicated that Fus3-mediated negative feedback acted downstream of mechanisms regulating G-protein association.

To confirm that Fus3 acted downstream of G-protein activation, we measured Ste5 recruitment after deleting *SST2*. We expected deletion of *SST2* to have no effect on Fus3-mediated signal decline, since Sst2 is required for efficient G-protein inactivation and, as we showed above, Fus3-mediated negative feedback does not reduce G-protein dissociation levels. Unexpectedly, when we deleted of *SST2*, we completely disrupted Fus3-mediated signal decline; unlike *SST2*+ cells, inhibition of Fus3 did not cause an increase in Ste5 recruitment (Fig. 4c). Furthermore, the Ste5 recruitment (with or without Fus3-mediated feedback) peaked and declined, similar to the baseline response of *SST2*+ cells (compare squares and circles in Fig. 4e with circles in Fig. 4c). This finding showed that signal peak-and-decline is the default behavior in the absence of Sst2. Since a sustained non-declining signal is only evident in *SST2*+ cells in the presence of Fus3-as2 inhibitor, these results also indicate that Sst2 promotes Ste5 membrane recruitment, a hitherto unknown function of the RGS protein family, and that Fus3 negatively regulates this novel signal-promoting function (Fig. 5a).

We then investigated which portions of the Sst2 protein might be involved in promoting Ste5 membrane recruitment. During analysis of Sst2 point mutants, we found that Ste5 recruitment in a *fus3-as2* strain that carried *sst2-T134A* instead of wild-type Sst2 peaked-

and-declined in the presence and absence of Fus3 inhibitor (Fig. 4f), just as observed in Δ*sst2* cells (Fig. 4e). The pheromone-induced growth-inhibition of *sst2-T134A* cells reported by halo assays was close to wild-type (Fig. S11a), and the average number of Sst2-T134A protein molecules per cell was similar to Sst2 abundance in the parent strain, (Fig. S11b), suggesting that the T134A mutation disrupted a significant fraction of the Fus3-dependent, signal-promoting function of Sst2 without disrupting the bulk of its signal-reducing GAP activity. T134 lies within the N-terminal DEP domains of Sst2, which are required for localization of Sst2 to the membrane by binding the cytosolic tail of Ste2 31. These results indicate that the DEP domains in Sst2 might aid Ste5 membrane recruitment, perhaps by providing additional membrane-proximal interaction surfaces, and suggest that mechanisms that regulate localization of Sst2 to the membrane, such as disruption of Sst2-Ste2 interactions by Yck1/2-mediated phosphorylation after longer periods of pheromone stimulation 31, might consequently regulate Ste5 membrane recruitment.

DoRA requires Fus3-mediated negative feedback

Finally, we tested if dose-response alignment between receptor-pheromone binding and downstream activities required Fus3 activity. In principle, Fus3-mediated negative feedback might scale system activity by a dose-independent factor, and therefore cause no shift in the normalized dose-response curve. For example, the Ste5 T287A mutation increases the magnitude of system output relative to wild-type cells without changing the pheromone concentration yielding half-maximal response (see Fig. 5 in 28). We measured dose-responses of Fus3 phosphorylation in a *fus3-as2* strain with and without inhibitor 15 minutes after pheromone stimulation, the time when the amount of Fus3 phosphorylation had declined to a steady-state level (Fig. 3c). Inhibiting Fus3 kinase activity shifted the dose-response of Fus3 activation, lowering the pheromone concentration needed for half maximal response by 20-fold (Fig. 5b). Moreover, inhibiting Fus3 kinase activity doubled the dynamic range of the output (Fig. 5c). These results showed that Fus3-mediated negative feedback was required for dose-response alignment in the yeast pheromone response system.

Discussion

We found that MAPK Fus3 mediates rapid negative feedback that aligns the dose-responses of upstream and downstream system activities in the pheromone response system. We propose that dose-response alignment improves information transmission through this and other signaling systems. Furthermore, we found that Fus3 negatively regulates a novel signal-promoting function of the RGS protein Sst2. Our results demonstrate that RGS proteins, present in many eukaryotic signaling systems (the human RGS family, for example, contains more than 35 members 32), can function in signal transduction systems by increasing signal in addition to accelerating G-protein inactivation, possibly (as in the case of pheromone response) by facilitating recruitment of MAPK scaffolds to sites of activity.

The idea that dose-response alignment increases the amount of transmitted information has practical implications for drug discovery and design. For example, consider a drug that increased sensitivity of cells to a naturally occurring antagonist of cell proliferation,

analogous to the downstream dose-response shift we observed upon Fus3 inhibition in the pheromone response system (Fig. 5b). Despite increasing the average sensitivity of cells to signals to stop growth, the dose-response misalignment could reduce the amount of transmitted information about the signal. The decrease in transmitted information could increase cell-to-cell variation in response, causing a larger number of cells fall below a threshold in antagonist response and continue proliferation. It is possible some existing drugs that allosterically modify GPCR signaling systems downstream of ligand binding (see 33, Fig. 3) and those that target mid-system signaling molecules such as PKC 34 and AKT 35 may decrease dose-response alignment and increase response variation, whereas drugs that specifically affect the affinity of receptor-ligand binding (see 33, Fig. 5) should not.

We propose here that the fidelity with which a cell responds to different input concentrations of a ligand depends on a “systems-level” quantitative behavior, dose-response alignment, found in many other cell signaling systems. For biological systems, a deeper understanding of key quantitative behaviors will likely depend on articulating appropriate analytical frameworks and metrics. Information theory36 defines a framework for quantifying the relationship between system input and output (see Supplementary Information 9 for further discussion), and has enabled researchers to quantify, for example, the amount of information that an axon of a single sensory neuron can transmit 37 and the amount of information about morphogen gradient that a transcription factor can transmit to a downstream effector 38,39. Much as concepts from classical electromagnetism provide rigorous means to describe and understand the determinants of behaviors of electrical circuits, we expect that concepts from information theory will enable more rigorous and quantitative understanding of how genes (and the proteins they encode) of more complicated signaling systems interact to sense and transmit information into the cell.

Methods Summary

We constructed yeast strains and plasmids by standard methods 40,41 essentially as described (5 and Supplementary Information 1). By doctrine, we expressed all reporter constructs from native promoters integrated into the chromosome, and verified that the level of expressed protein was similar to the native level. With the exception of strains used for G-protein FRET experiments, we constructed all strains were from otherwise- isogenic *bar1*-W303a reference parent strain, ACL 379 5, by the steps described. We stimulated exponentially-growing cells with the indicated concentration of pheromone and/or other reagents (such as the inhibitor 1-NM-PP1) in one of two ways. For image cytometry, we affixed the cells to the bottom of wells in a glass-bottom 96-well plate, as described in 5 and in Supplementary Information 2.1. Using custom fluidic hardware, we evacuated medium from the well, injected fresh medium containing the indicated concentration of pheromone and/or inhibitor, and proceeded to record images over time. For MAPK phosphorylation, *FUS1* mRNA, and flow cytometry experiments, we stimulated cells by using a micropipette to mix a small volume of pheromone and/or inhibitor into the cell suspension to the final concentration (as indicated, typically 100 nM pheromone and 10 μM 1-NM-PP1). We performed image acquisition essentially as described in 5,23, with modifications as detailed in Supplementary Information. For image cytometry, we extracted values for parameters of interest from images using Cell-ID 1.0 23. We analyzed image and flow cytometric data

using Physics Analysis Workstation (PAW; see 42) and custom scripts, depending on the type of image, described in the text and in Supplementary Information. Supplementary Information contains further details on plasmids, strains, construction methods, materials, and experimental methods.

Supplementary Material

Refer to Web version on PubMed Central for supplementary material.

Acknowledgments

We thank Pia Abola, Steven Andrews, Adam Arkin, Mark Bowen, Linda Buck, Charles Denby, Alexander Gann, Deidre Meldrum, Tim Mitchison, Carl Pabo, Mark Ptashne, Michael Reese, Orna Resnekov, Chris Ryan, Michael Snyder, Ty Thomson, Annie E. Tsong, and Mark Wilson for discussions and/or comments on the manuscript, and Orna Resnekov for help in articulating the requirements for fluidic induction devices. Work, including that of Mark Holl at U. Washington, was supported by the Alpha Project at the Center for Quantitative Genome Function, an NIH Center of Excellence in Genomic Science under grant P50 HG02370 from the National Human Genome Research Institute to R.B.

References

1. Dohlman HG, Thorner JW. Regulation of g protein-initiated signal transduction in yeast: Paradigms and principles. Annu Rev Biochem. 2001; 70:703–754. [PubMed: 11395421]
2. Jackson CL, Hartwell LH. Courtship in s. Cerevisiae: Both cell types choose mating partners by responding to the strongest pheromone signal. Cell. 1990; 63:1039–1051. [PubMed: 2257622]
3. Segall JE. Polarization of yeast cells in spatial gradients of alpha mating factor. Proc Natl Acad Sci U S A. 1993; 90:8332–8336. [PubMed: 8397402]
4. Schrick K, Garvik B, Hartwell LH. Mating in saccharomyces cerevisiae: The role of the pheromone signal transduction pathway in the chemotropic response to pheromone. Genetics. 1997; 147:19–32. [PubMed: 9286665]
5. Colman-Lerner A, Gordon A, Serra E, Chin T, Resnekov O, Endy D, et al. Regulated cell-to-cell variation in a cell-fate decision system. Nature. 2005; 437:699–706. [PubMed: 16170311]
6. Yi TM, Kitano H, Simon MI. A quantitative characterization of the yeast heterotrimeric g protein cycle. Proc Natl Acad Sci U S A. 2003; 100:10764–10769. [PubMed: 12960402]
7. Cuatrecasas P. Insulin--receptor interactions in adipose tissue cells: Direct measurement and properties. Proc Natl Acad Sci U S A. 1971; 68:1264–1268. [PubMed: 5288373]
8. Kasai M, Changeux JP. In vitro excitation of purified membrane by cholinergic agonists. J Membrane Biol. 1971; 6:58. [PubMed: 24173289]
9. Amir SM, Carraway TF Jr, Kohn LD, Winand RJ. The binding of thyrotropin to isolated bovine thyroid plasma membranes. J Biol Chem. 1973; 248:4092–4100. [PubMed: 4122527]
10. Lin SY, Goodfriend TL. Angiotensin receptors. The American journal of physiology. 1970; 218:1319–1328. [PubMed: 4314569]
11. Knauer DJ, Wiley HS, Cunningham DD. Relationship between epidermal growth factor receptor occupancy and mitogenic response. Quantitative analysis using a steady state model system. J Biol Chem. 1984; 259:5623–5631. [PubMed: 6325444]
12. Nagashima T, Shimodaira H, Ide K, Nakakuki T, Tani Y, Takahashi K, et al. Quantitative transcriptional control of erbb receptor signaling undergoes graded to biphasic response for cell differentiation. J Biol Chem. 2007; 282:4045–4056. [PubMed: 17142811]
13. Simons SS Jr, Oshima H, Szapary D. Higher levels of control: Modulation of steroid hormone-regulated gene transcription. Molecular endocrinology (Baltimore, Md. 1992; 6:995–1002.
14. Rousseau GG, Baxter JD. Glucocorticoid receptors. Monogr Endocrinol. 1979; 12:49–77. [PubMed: 386089]

15. Bloom E, Matulich DT, Lan NC, Higgins SJ, Simons SS, Baxter JD. Nuclear binding of glucocorticoid receptors: Relations between cytosol binding, activation and the biological response. Journal of steroid biochemistry. 1980; 12:175–184. [PubMed: 7421206]
16. Pedraza JM, van Oudenaarden A. Noise propagation in gene networks. Science. 2005; 307:1965–1969. [PubMed: 15790857]
17. Black HS. Stabilized feed-back amplifiers. Electrical Engineering. 1934; 53:114–120.
18. Bhalla US, Ram PT, Iyengar R. Map kinase phosphatase as a locus of flexibility in a mitogen-activated protein kinase signaling network. Science. 2002; 297:1018–1023. [PubMed: 12169734]
19. Black JW, Leff P. Operational models of pharmacological agonism. Proc R Soc Lond B Biol SciI. 1983; 220:141–162.
20. Savageau MA. Comparison of classical and autogenous systems of regulation in inducible operons. Nature. 1974; 252:546–549. [PubMed: 4431516]
21. Becskei A, Serrano L. Engineering stability in gene networks by autoregulation. Nature. 2000; 405:590–593. [PubMed: 10850721]
22. Barkai N, Leibler S. Robustness in simple biochemical networks. Nature. 1997; 387:913–917. [PubMed: 9202124]
23. Gordon A, Colman-Lerner A, Chin TE, Benjamin KR, Yu RC, Brent R. Single-cell quantification of molecules and rates using open-source microscope-based cytometry. Nat Methods. 2007; 4:175–181. [PubMed: 17237792]
24. Gartner A, Nasmyth K, Ammerer G. Signal transduction in saccharomyces cerevisiae requires tyrosine and threonine phosphorylation of fus3 and kss1. Genes Dev. 1992; 6:1280–1292. [PubMed: 1628831]
25. Tedford K, Kim S, Sa D, Stevens K, Tyers M. Regulation of the mating pheromone and invasive growth responses in yeast by two map kinase substrates. Curr Biol. 1997; 7:228–238. [PubMed: 9094309]
26. Miyawaki A, Tsien RY. Monitoring protein conformations and interactions by fluorescence resonance energy transfer between mutants of green fluorescent protein. Methods Enzymol. 2000; 327:472–500. [PubMed: 11045004]
27. van Drogen F, Stucke VM, Jorritsma G, Peter M. Map kinase dynamics in response to pheromones in budding yeast. Nat Cell Biol. 2001; 3:1051–1059. [PubMed: 11781566]
28. Bhattacharyya RP, Remenyi A, Good MC, Bashor CJ, Falick AM, Lim WA. The ste5 scaffold allosterically modulates signaling output of the yeast mating pathway. Science. 2006; 311:822–826. [PubMed: 16424299]
29. Gruhler A, Olsen JV, Mohammed S, Mortensen P, Faergeman NJ, Mann M, et al. Quantitative phosphoproteomics applied to the yeast pheromone signaling pathway. Mol Cell Proteomics. 2005; 4:310–327. [PubMed: 15665377]
30. Bishop AC, Ubersax JA, Petsch DT, Matheos DP, Gray NS, Blethrow J, et al. A chemical switch for inhibitor-sensitive alleles of any protein kinase. Nature. 2000; 407:395–401. [PubMed: 11014197]
31. Ballon DR, Flanary PL, Gladue DP, Konopka JB, Dohlman HG, Thorner J. Dep-domain-mediated regulation of gpcr signaling responses. Cell. 2006; 126:1079–1093. [PubMed: 16990133]
32. Heximer SP, Blumer KJ. Rgs proteins: Swiss army knives in seven-transmembrane domain receptor signaling networks. Sci STKE. 2007; 2007:pe2. [PubMed: 17244887]
33. May LT, Leach K, Sexton PM, Christopoulos A. Allosteric modulation of g protein-coupled receptors. Annual review of pharmacology and toxicology. 2007; 47:1–51.
34. Budas GR, Churchill EN, Mochly-Rosen D. Cardioprotective mechanisms of pkc isozyme-selective activators and inhibitors in the treatment of ischemia-reperfusion injury. Pharmacol Res. 2007; 55:523–536. [PubMed: 17576073]
35. Lindsley CW, Barnett SF, Layton ME, Bilodeau MT. The pi3k/akt pathway: Recent progress in the development of atp-competitive and allosteric akt kinase inhibitors. Current cancer drug targets. 2008; 8:7–18. [PubMed: 18288939]
36. Shannon C. A mathematical theory of communication. Bell System Technical Journal. 1948; 27:379–423.

37. Bialek W, Rieke F, de Ruyter van Steveninck RR, Warland D. Reading a neural code. Science. 1991; 252:1854–1857. [PubMed: 2063199]

38. Tkacik G, Calan C, Bialek W. Information flow and optimization in transcriptional control. Phys Rev E. 2008 In press.

39. Gregor T, Tank DW, Wieschaus EF, Bialek W. Probing the limits to positional information. Cell. 2007; 130:153–164. [PubMed: 17632062]

40. Ausubel, FM.; Brent, R.; Kingston, RE.; Moore, DD.; Seidman, JG.; Smith, JA., et al. Current protocols in molecular biology. John Wiley & Sons, Inc.; New York, N.Y.: 1987–2006.

41. Guthrie, C.; Fink, GR. Methods in enzymology, guide to yeast genetics and molecular biology. Academic Press; San Diego, California 92101: 1991.

42. Brun R, Couet O, Vandroni C, Zanarini O. Paw physics analysis workstation cern program library entry q121. CERN Geneva. 1989

43. Jenness DD, Burkholder AC, Hartwell LH. Binding of alpha-factor pheromone to saccharomyces cerevisiae a cells: Dissociation constant and number of binding sites. Mol Cell Biol. 1986; 6:318–320. [PubMed: 3023832]

44. Bajaj A, Celic A, Ding FX, Naider F, Becker JM, Dumont ME. A fluorescent alpha-factor analogue exhibits multiple steps on binding to its g protein coupled receptor in yeast. Biochemistry. 2004; 43:13564–13578. [PubMed: 15491163]

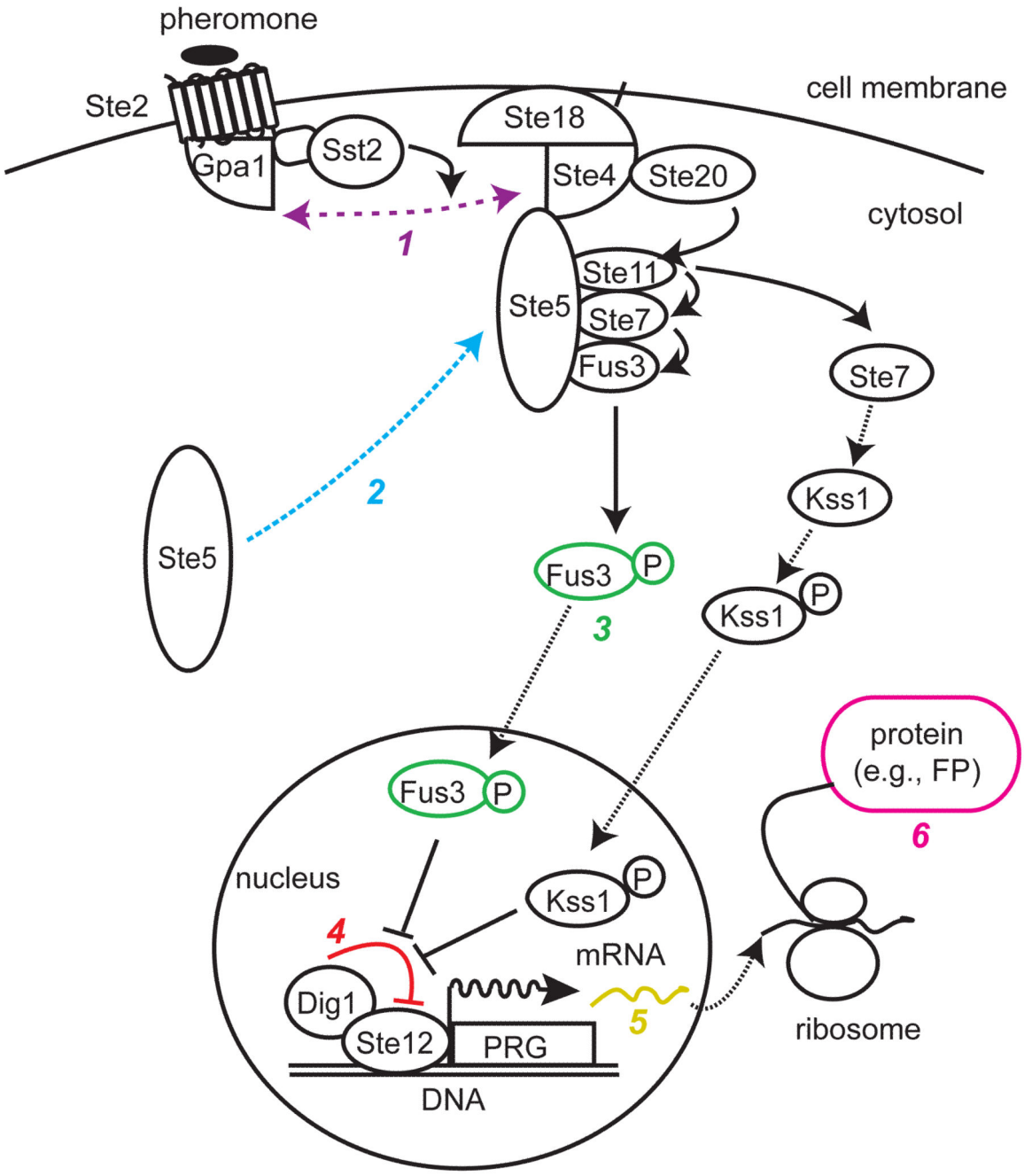

Figure 1. The pheromone response system

Proteins are indicated by labeled ovals, translocation by dotted lines, protein activation by arrows, inhibition by T-bar arrows, and protein association by double-headed dashed arrows. Pheromone binding by receptor Ste2 causes dissociation of the heterotrimeric G-protein (1) into G_{α} subunit (Gpa1) and the $G_{\beta\gamma}$ dimer (Ste4-Ste18). GTP-activating protein (GAP) function of the Regulator of G-protein Signaling (RGS)-protein Sst2 promotes re-association of Gpa1 with Ste4-Ste18. Upon dissociation of the G-protein, Ste4 helps recruit the MAP kinase scaffold Ste5 to the membrane (2). Ste5 recruitment activates of the MAP kinase

cascade, in which Ste20, Ste11, Ste7, and the MAP kinases Fus3 and Kss1 phosphorylate one another in sequence. Phosphorylated Fus3 (3) translocates to the nucleus and phosphorylates Dig1 and Ste12, eliminating Dig1 repression of Ste12, a transcriptional activator (4). Ste12 activates transcription of pheromone responsive genes (PRGs) (5,6).

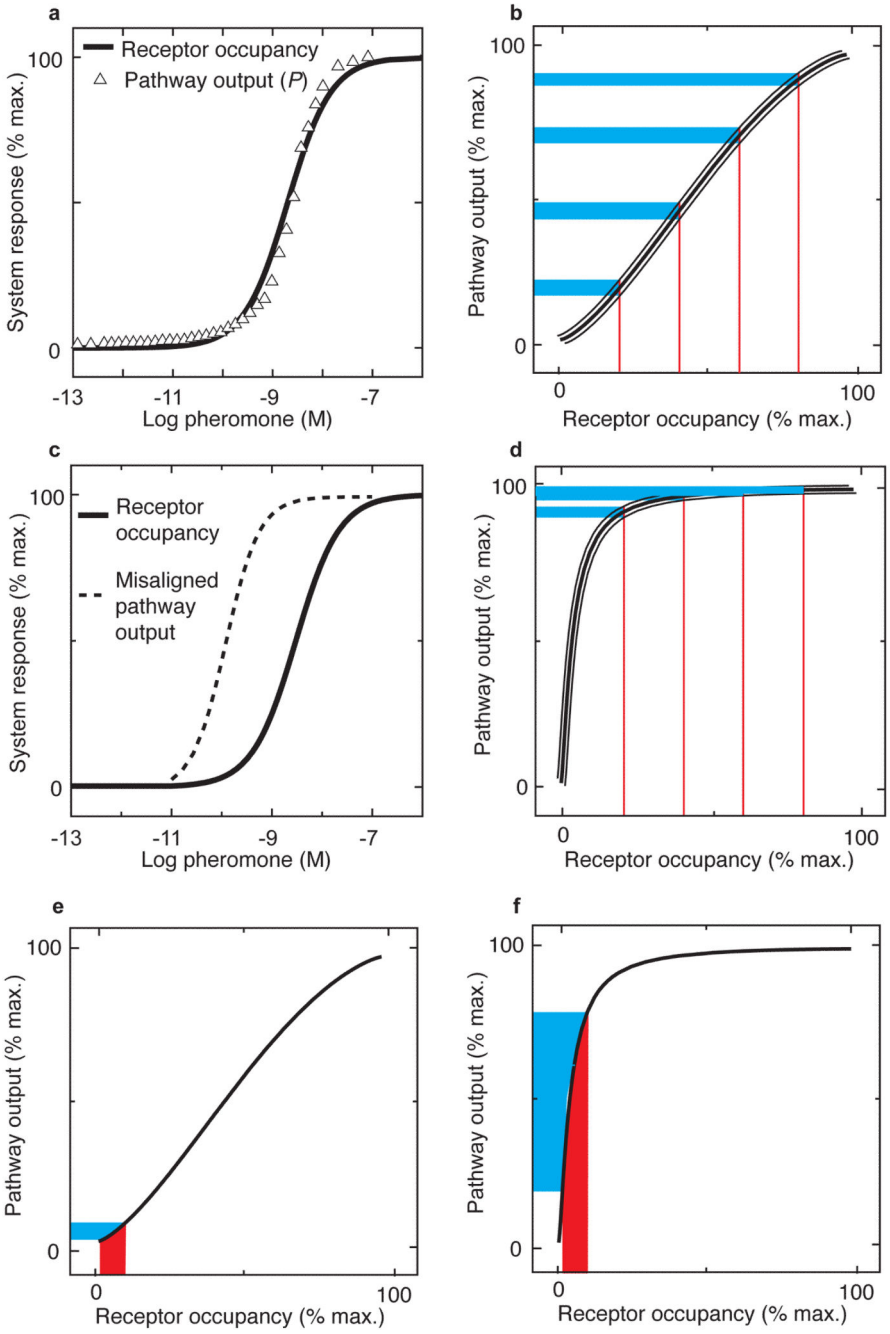

Figure 2. DoRA increases response distinguishability

a) Dose-responses of receptor occupancy (calculated from reported receptor-pheromone binding affinity measurements 43,44) and reporter gene expression output corrected for known sources of cell-to-cell variation (pathway output P 5), align closely.

b) Relationship between receptor occupancy and downstream response (from panel a) is essentially linear. Evenly-distributed receptor occupancies (20 %, 40 %, 60 %, and 80 %, red vertical lines) corresponded to evenly-spaced downstream responses (blue horizontal lines).

c) Example of dose-response misalignment, in which the downstream output is 20-fold more sensitive than that in panel a (i.e., the EC50 is reduced 20-fold).
d) Dose-response misalignment makes transfer function non-linear, which compresses the downstream responses (blue horizontal lines) corresponding to the majority of receptor occupancies (red vertical lines), reducing downstream response distinguishability.
e,f) Dose-response misalignment results in noise amplification. Receptor occupancy (red vertical line) with some noise (pink spread) yields downstream responses (horizontal dotted lines) with associated noise (spread around horizontal blue bars). In system with DoRA (e), linear transfer function yields less noise in downstream response than in system with misaligned dose-responses and non-linear transfer function (f).

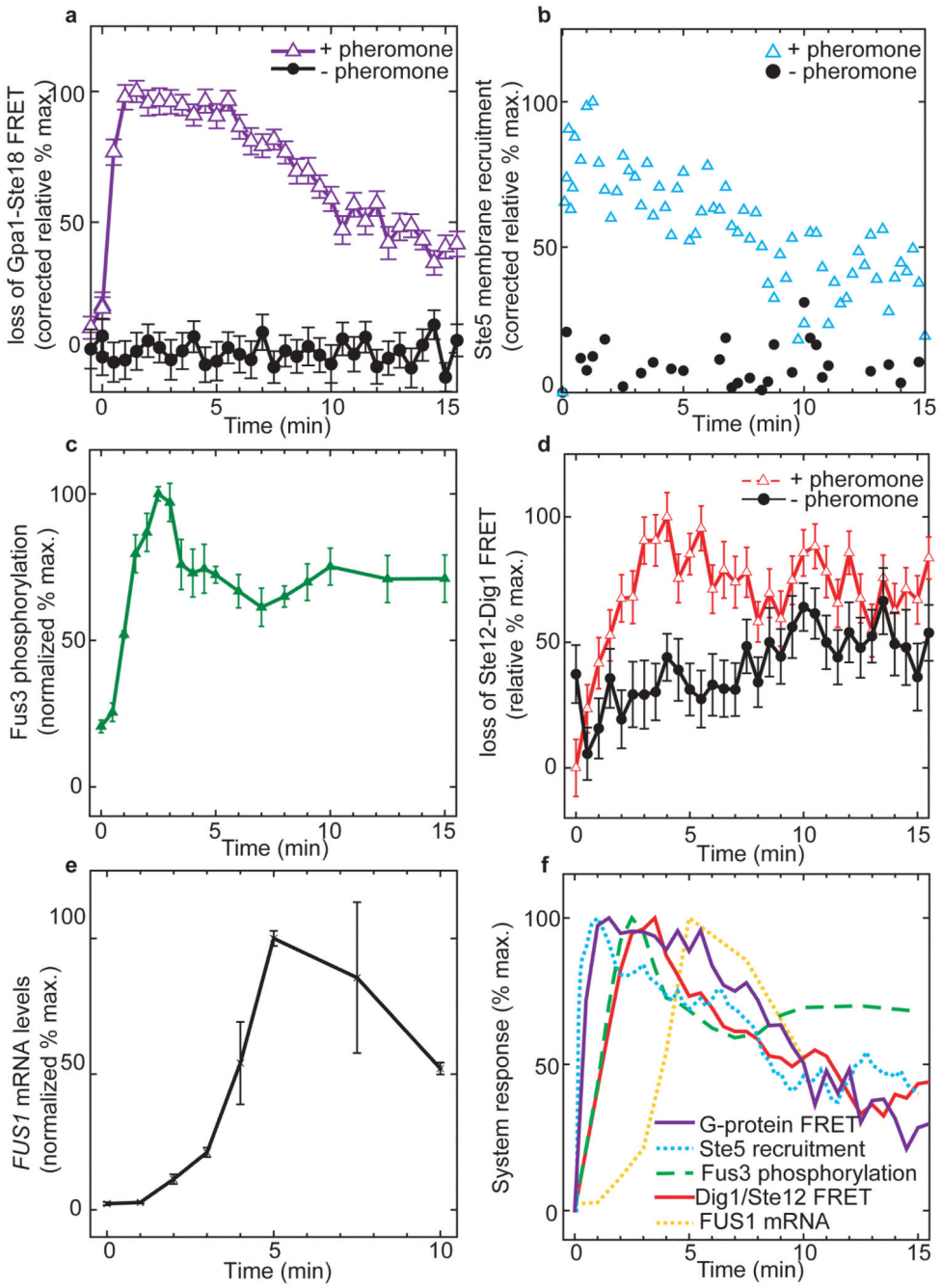

Figure 3. Initial system dynamics indicate negative feedback

a) Loss of G-protein FRET. Corrected median (+/− SE) loss of Gpa1-Ste18 FRET values (relative to maximum change measured in pheromone-stimulated cells; see Fig. S2) in RY2062b cells stimulated with pheromone (open purple triangles; n=262) quickly peaked and declined to a plateau relative to unstimulated cells (black circles; n=143).

b) YFP-Ste5 recruitment. Corrected median (+/− SE) YFP-Ste5 membrane recruitment (relative to maximum change measured in pheromone-stimulated cells; see Fig. S3e) in

RY2013 cells stimulated with pheromone stimulation (open cyan triangles, n=361) quickly peaked and declined to a plateau compared to unstimulated cells (black circles, n=223).
c) Fus3 activity. Mean ratios (+/− S.E., n=3–5) of activated (phospho-Y180 and phospho-T182) Fus3 to total Fus3, normalized to the peak measured ratio (see Fig. S4 for representative immunoblot images). Fus3 activity levels peaked 2.5 minutes after pheromone stimulation and declined to a plateau within 5 minutes of stimulation. Total Fus3 levels, compared to levels of non-pheromone regulated proteins GAPDH and PGK1, remained constant over this time period (data not shown). New protein synthesis is not required for the observed peak and decline (Fig. S4c).
d) Loss of Dig1-Ste12 FRET. Median (+/− SE) loss of Dig1-Ste12 FRET (scaled to minimum and maximum values for measured in pheromone-stimulated cells; for raw values, see Fig. S7) in RY1130b cells peaked about 3 minutes following pheromone stimulation, and then declined to a plateau (open red triangles, n=246) relative to unstimulated cells (black circles, n=138).
e) *FUS1* mRNA. Average ratio (high/low values indicated) of *FUS1* mRNA probe band intensity to loading control (*ACT1* mRNA probe band intensity) after pheromone stimulation (filled squares, n=2) (See Fig S8 for raw image).
f) Composite timing plot shows persistent peak-and-decline toward a plateau for all system responses, suggesting action of negative feedback. YFP-Ste5 recruitment and Dig1/Ste12 FRET (from panels b and d) were smoothed using a moving window of five data points.

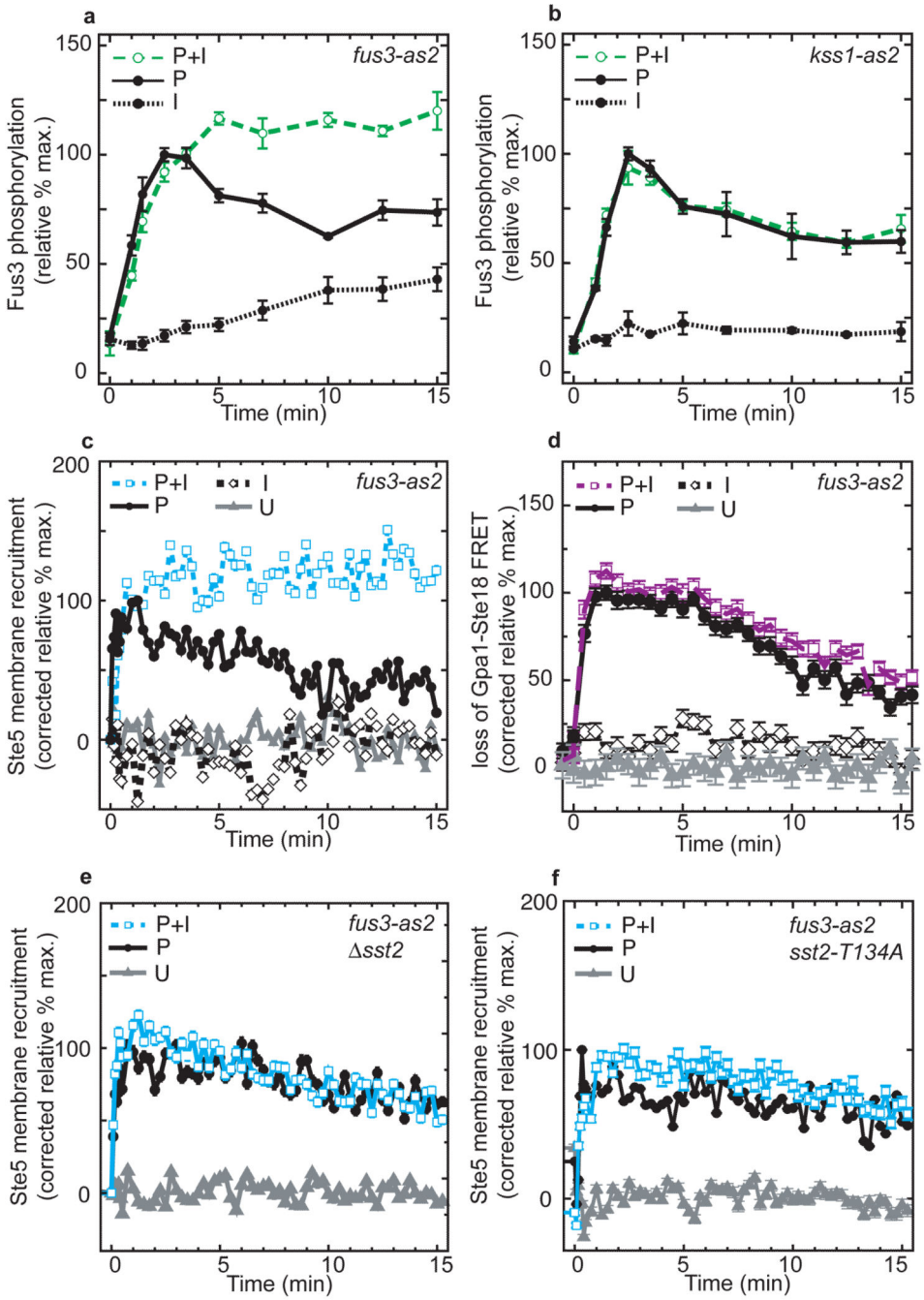

Figure 4. Fus3 mediates negative feedback

Values scaled to peak signal measured in cells stimulated with only pheromone. Error bars indicate +/− SE. For all panels: P, stimulated with 100 nM pheromone; P+I, stimulated with 100 nM pheromone + 10 μM 1-NM-PP1; I, 10 μM 1-NM-PP1; U, untreated.

a) Fus3 mediates negative feedback. In *fus3-as2* cells (RY1134b), mean (n=4) Fus3 phosphorylation peaked and declined, as in *FUS3* cells (Fig. 3b), after pheromone stimulation (black circles), but did not decline when we stimulated cells simultaneously with

Fus3-as2 inhibitor (open green circles). Treating cells with only inhibitor (gray circles) caused the signal to slowly rise, indicating cells actively regulate basal signal level.
b) Kss1 does not mediate negative feedback. In *kss1-as2* cells (RY1133b), mean (n=4) Fus3 phosphorylation in pheromone-stimulated cells without (black circles) or with (open green circles) simultaneous treatment with Kss1-as2 inhibitor were identical. Treating cells with only inhibitor caused no significant increase in Fus3 phosphorylation (gray circles).
c) Fus3-mediated feedback acts on or upstream of Ste5 membrane recruitment. In *fus3-as2* cells (RY2013), median YFP-Ste5 membrane recruitment peaked and declined after pheromone stimulation (filled circles; n=361), but did not decline after simultaneous treatment with Fus3-as2 inhibitor (n=196, open blue squares). There was no relative Ste5 recruitment in cells treated with inhibitor alone (open diamonds; n=134) or in completely untreated cells (gray triangles; n>100). The small increase in Fus3 phosphorylation measured in cells treated with inhibitor only (black circles in Fig. 4a) suggests that additional Fus3-independent mechanisms maintain low basal levels of Ste5 recruitment.
d) Fus3-mediated negative feedback acts downstream of G-protein dissociation. In *fus3-as2* cells (RY2062b, derived from TMY101 6), median Gpa1-Ste18 loss of FRET peaked and declined in pheromone-stimulated cells (filled circles; n=262) with the same dynamics as in pheromone-stimulated cells simultaneously treated with Fus3-as2 inhibitor (open purple squares; n=263). Unstimulated cells in the presence (open diamonds; n=229) or absence (gray triangles n=143) of inhibitor showed no loss of Gpa1-Ste18 FRET.
e) One target of Fus3-mediated negative feedback is a novel Sst2-dependent increases in YFP-Ste5 recruitment. Median YFP-Ste5 membrane recruitment in pheromone-stimulated *fus3-as2* Δ*sst2* cells (RY2024) peaked and declined both in the absence (black circles; n=188) or presence (open cyan squares; n=300) of Fus3-as2 inhibitor, similar to *SST2* cells with active Fus3 (black circles, panel (c)). Unstimulated cells, gray triangles (n>100).
f) Mutation of predicted Fus3/MAPK phosphorylation site in Sst2 DEP1 domain eliminated Sst2 promotion of YFP-Ste5 recruitment. Median (+/− SE) YFP-Ste5 membrane recruitment in pheromone-stimulated *sst2-T134A* (RY2066) cells peaked and declined both in the absence (filled circles; n>150) and presence (open cyan squares; n>150) of inhibitor, similar to Δ*sst2* cells (Fig. 4e).

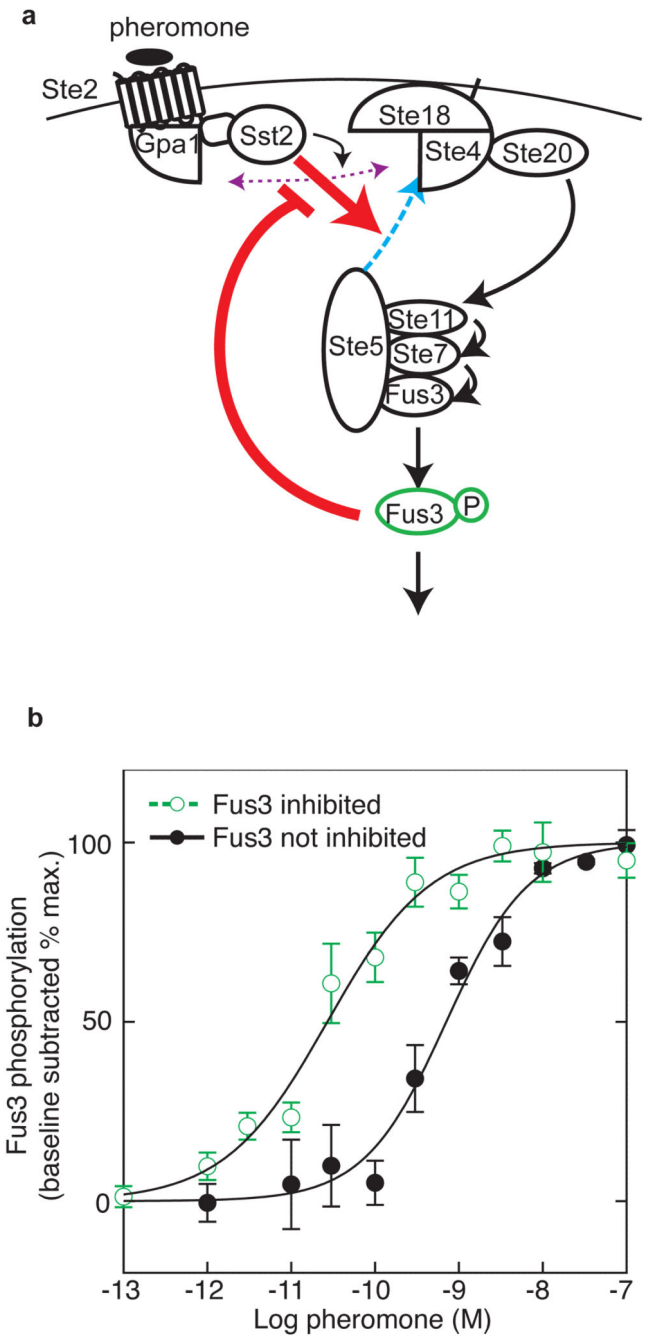

Figure 5. DoRA requires Fus3-mediated negative feedback

a) Model of negative feedback regulation of Ste5 membrane recruitment. Sst2 promotes (thick red arrow) Ste5 recruitment to the membrane (blue dashed arrow), and Fus3 negatively regulates this signal promotion (thick T-bar arrow).

b) Fus3 inhibition disrupts dose-response alignment. In pheromone-stimulated *fus3-as2* (RY2052b) cells, inhibition of Fus3 kinase activity (open green circles) reduced the sensitivity (EC50) of the dose response of mean Fus3 phosphorylation (+/− SE; n=3–4) relative to cells not treated with inhibitor (black filled circles). Fus3 phosphorylation

measured after 15 minutes of pheromone stimulation, after the signal reaches the dose-dependent plateau (see Fig. 3c). Black lines show fits to Hill functions. Fus3 inhibition reduced the EC50 of the dose-response by greater than 20 fold without affecting the gradedness (cooperativity) of the average response (see Supplementary Information for details).